EuroIntervention
2025;21:e1028-e1036
published online e-edition September 2025
DOI: 10.4244/EIJ-D-25-00349

ORIGINAL RESEARCH

A preclinical study of combined hepatic and renal artery denervation

Felix Mahfoud[1]*, MD; Stefan Tunev[2], DVM; David E. Kandzari[3], MD; Eric A. Secemsky[4], MD; Pam R. Taub[5], MD; Raven A. Voora[6], MD; Lucas Lauder[1], MD; Cian Ryan[2], BEng; Julie Trudel[2], PhD; Douglas A. Hettrick[2], PhD; Markus Schlaich[7], MD

**Corresponding author: Department of Cardiology, University Heart Center, Petersgraben 4, 4031, Basel, Switzerland. E-mail: felix.mahfoud@usb.ch*

This paper also includes supplementary data published online at: https://eurointervention.pcronline.com/doi/10.4244/EIJ-D-25-00349

ABSTRACT

BACKGROUND: Overactivity of the hepatic and renal sympathetic nerves is associated with chronic cardiovascular and metabolic conditions, including hypertension.

AIMS: We studied the effect of combined renal and hepatic denervation through treatment of the common hepatic artery and the renal arteries.

METHODS: Denervation was performed in the common hepatic artery and both renal arteries and their major branch vessels in normotensive swine using the same multielectrode radiofrequency (RF) ablation catheter (Symplicity Spyral). Renal and liver tissue samples were obtained for histological examination in two cohorts at 7 and 28 days post-procedure (n=5 sham, n=10 denervation for each timepoint).

RESULTS: Combined hepatic and renal denervation was successfully achieved in all animals. At 7 days, the mean lesion depth was 5.8±1.4 mm in the renal arteries and 4.7±0.7 mm in the hepatic artery. Compared with controls, the mean renal cortical norepinephrine (NE) levels were reduced by 88.2% in the 7-day model and by 84.5% in the 28-day model. Liver NE decreased by 94.6% at 7 days and by 91.1% at 28 days ($p<0.0001$ for all comparisons with baseline). No inadvertent injury was detected in the treated arteries or adjacent tissues.

CONCLUSIONS: Combined hepatic and renal denervation using the same multielectrode RF denervation system resulted in a substantial reduction in both renal and hepatic tissue NE levels that was sustained up to 28 days without collateral tissue injury. These mechanistic findings may have implications for the treatment of chronic diseases impacted by hepatic and renal sympathetic nervous system overactivity.

KEYWORDS: ablation; hepatic denervation; hypertension; radiofrequency; renal denervation; sympathetic nervous system

SUBMITTED ON 02/04/2025 - REVISION RECEIVED ON 09/05/2025 - ACCEPTED ON 19/05/2025

Modulation of the autonomic nervous system via percutaneous radiofrequency (RF) renal denervation (RDN) has been shown to safely and durably lower blood pressure (BP) in patients with uncontrolled hypertension and is an approved and guideline-recommended therapy in multiple countries[1-3]. However, not all patients receiving the procedure experience substantial BP reductions, and predictors of treatment response are inconsistent. Therefore, a clinical need exists to safely amplify the efficacy of autonomic modulating procedures. Similar to the kidneys, the human liver is richly innervated by the sympathetic nerves, presenting an additional opportunity to attenuate organ-specific sympathetic activity[4]. Preliminary physiological and anatomical studies have examined the common hepatic artery (CHA) as a promising target for additional interventions due to its dense sympathetic innervation within close proximity to the vessel lumen[5,6]. A catheter-based approach to CHA denervation could provide an opportunity to augment the BP response to RDN therapy in hypertensive patients. Many hypertensive patients also experience comorbidities that may be influenced by autonomic modulation, including those with metabolic syndrome, type 2 diabetes, and metabolic dysfunction-associated steatotic liver disease (MASLD)[7]. In this preclinical model, we studied the feasibility and safety of combined RF treatment of the CHA and the renal arteries and its effect on tissue-specific sympathetic activity using the same approved multielectrode RF catheter system.

Impact on daily practice

Renal denervation is a guideline-recommended therapy for patients with uncontrolled hypertension. Expansion of denervation beyond the renal arteries to the common hepatic artery may improve blood pressure response as well as impact other cardiometabolic disorders. The present preclinical results demonstrate that multiorgan denervation is feasible using the same system within the same procedure and establish a pathway to first-in-human clinical trials.

Methods

Predefined studies were performed in accordance with the Guide for the Care and Use of Laboratory Animals of the National Institutes of Health (Publication Number 85-23, revised 1996), in compliance with the Animal Welfare Act and the U.S. Food and Drug Administration (FDA) regulations and their amendments.

Yorkshire domestic farm swine (N=30) weighing between 35 kg and 50 kg were assigned to 2 groups for histological study at 7 days (group 1; n=10) and 28 days (group 2; n=10) **(Figure 1)**. Two separate groups (each n=5) underwent angiography only and served as concomitant controls. All procedures were performed during general anaesthesia and via femoral access. Arterial dimensions were determined using quantitative vascular analysis (QVA). The multielectrode RF catheter (Symplicity Spyral [Medtronic]) was advanced through a guiding catheter and sequentially into the right and left renal arteries and into the CHA via the coeliac trunk under fluoroscopic guidance **(Figure 2)**. Two 60-second RF energy applications were sequentially delivered via 4 catheter electrodes to the main renal arteries. An additional treatment cycle, including up to 4 lesions, was performed in the primary inferior and superior left and right renal artery branch vessels. Next, two sequential applications of up to 8 lesions in total were delivered to the CHA in the distal and proximal locations, respectively. A single catheter device was used for all RF treatments in each animal.

Following euthanasia, a complete necropsy was performed on all animals and any gross abnormalities were recorded. The bilateral renal arteries were harvested *en bloc* along with the surrounding tissues, including the adrenal glands, psoas muscles, ureters, lymph nodes, and kidneys. The common hepatic artery was similarly collected *en bloc* with adjacent tissues, including the coeliac trunk, lymph nodes, pancreas, portal veins, bile duct, and adjacent liver. All specimens were fixed in 10% neutral buffered formalin (NBF). In addition, the left lateral, left medial, right lateral, and right medial lobes of the liver, as well as any gross lesions identified during necropsy or tissue removal not included in the *en bloc* samples, were separately collected and fixed in 10% NBF. Serial histological tissue samples of the common hepatic and both renal arteries and surrounding tissues were obtained for each group at 7 and 28 days post-procedure, as previously described[8]. Briefly, the arterial tree was serially sectioned every 3-4 mm along the longitudinal axis to generate up to 28 individual tissue sections per vessel in the renal arteries and up to 18 levels per hepatic artery. Each tissue slice was subclassified according to its relative position in the vessel including proximal, main, branch, and distal sections to account for variability in the length of the individual vessels between animals. Renal arteries were treated in the main and first order branches, whereas the hepatic artery was treated only in the main CHA between the splenic and gastroduodenal artery branching points. Each slide was stained with haematoxylin and eosin. Necrosis was identified by obliteration of nerve structure, presence of nerve cell debris, hypercellularity, loss of blood vessels, and transformation to phagocytic Schwann cell phenotype. Fibrosis was characterised by disruption of normal nerve structure, visible fibrosis, and hypercellularity. A pathologist blinded to the gross tissue-sectioning process assessed the presence of vascular endothelialisation, tissue necrosis, fibrosis and distal nerve bundle atrophy (axonal loss) for each tissue section using an established[9-11] semiquantitative scale of 0-4 including both ablated and non-ablated regions **(Supplementary Table 1)**. Each section was scored individually

Abbreviations

BP	blood pressure	**NE**	norepinephrine
CHA	common hepatic artery	**QVA**	quantitative vascular analysis
MASLD	metabolic dysfunction-associated steatotic liver disease	**RDN**	renal denervation
NBF	neutral buffered formalin	**RF**	radiofrequency

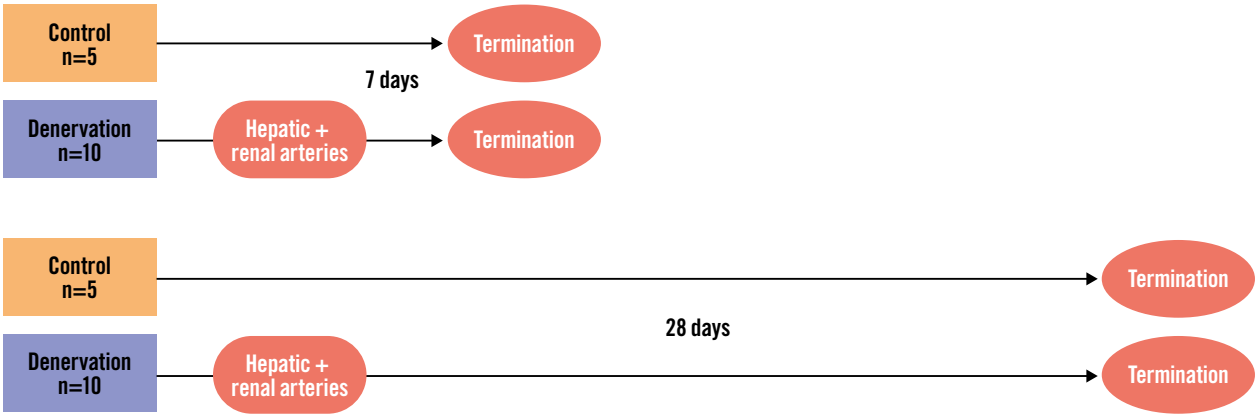

Figure 1. *Study block diagram. Normotensive swine were treated with both renal and common hepatic denervation. Tissue samples were analysed in separate cohorts at 7 and 28 days post-procedure. Control animals received angiography only.*

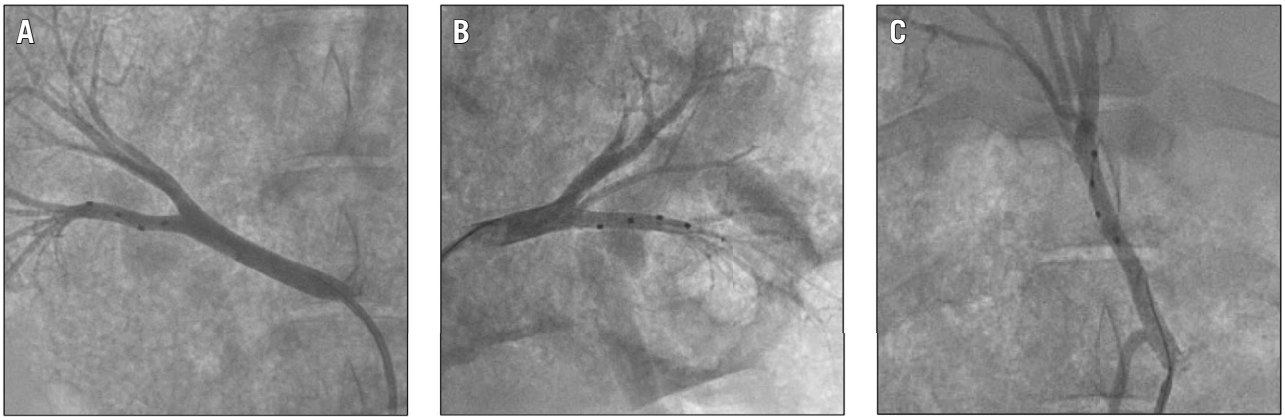

Figure 2. *Fluoroscopy images of the renal and hepatic denervation procedure. Example fluoroscopic images of the multielectrode radiofrequency Symplicity Spyral catheter in the right (A) and left (B) renal arteries as well as in the common hepatic artery (C).*

and scores within each were averaged according to the relative positioning of the section. Norepinephrine (NE) content was determined on treated and untreated kidney and liver tissue samples using high-performance liquid chromatography as described previously[8,9,12].

The lesion depth for each histological section was defined as the maximal perpendicular distance from the outer edge of the vessel wall to the furthest border of detectable tissue damage. The "mean lesion depth" was calculated as the average of all depth measurements from all histological samples for a single vessel. The maximum lesion depth was determined as the greatest mean lesion depth for each vessel averaged across all vessels. The maximum circumferential extension of perivascular ablation was defined as the highest relative circumferential proportion of extravascular tissue damage of any sample of the treated vessel **(Supplementary Figure 1)**. The mean circumferential extension of perivascular ablation was defined as the average of all circumferential proportions for all samples in a single vessel.

STATISTICAL ANALYSIS

Each animal contributed two kidneys for analysis since RDN was performed bilaterally. Data are reported as mean±standard deviation (SD) or 95% confidence interval and range as indicated. Differences in NE concentration were evaluated using unpaired Student's t-tests with Welch's correction. Variability in tissue NE between the kidney and liver samples was compared via the F-test. All p-values were two-sided, and values obtained from different tissues of the same animal were considered independent. A p-value of <0.05 was considered significant.

Results

Combined hepatic and bilateral renal denervation were successfully achieved in all test animals in the 7-day and 28-day groups (n=5 control, n=10 denervation for both groups). The average times from procedure to termination were 7±1 days and 28±2 days, respectively. Renal main and branch and hepatic artery dimensions (QVA) are shown in **Table 1**. The mean renal artery diameter including both studies was 6.6±0.7 mm and 6.5±0.6 mm for the left and right renal arteries, respectively, while the mean diameter of the common hepatic artery was 5.3±0.4 mm. The depth of RF tissue damage was significantly greater at 7 days than at 28 days in the renal arteries but not in the CHA **(Table 2)**. The maximal perivascular ablation

Table 1. Renal and hepatic arteries' diameter and length.

	Left renal artery			Right renal artery			Common hepatic artery
	Main	Inferior	Superior	Main	Inferior	Superior	
Diameter, mm	6.6±0.7	4.3±0.5	4.5±0.8	6.5±0.6	4.3±0.6	4.5±0.7	5.3±0.4
Length, mm	20.0±5.9	23.6±6.4	19.7±6.0	33.7±5.6	22.6±6.9	18.0±6.4	51.0±8.5

Data are mean±standard deviation. N=20. Branch artery length is determined from main bifurcation to kidney shadow.

Table 2. Radiofrequency lesion depth and circumferential extension in renal and common hepatic arteries.

		N	Lesion depth		Circumferential extension	
			Mean, mm	Max, mm	Mean, %	Max, %
Renal	7 days	20	5.8±1.4	10.6±3.0	33.0±7.2	59.0±18.7
	28 days	20	4.1±1.4*	7.7±3.0*	35.3±11.3	67.3±19.7
Hepatic	7 days	10	4.7±0.7	7.1±1.3	37.0±15.6	59.5±22.9
	28 days	10	4.4±0.6	6.9±1.1	43.2±7.3	73.0±7.5

Data are mean±standard deviation. *p<0.01 vs 7 days

circumferential extension was ≥59% in both renal and hepatic samples.

Compared to control, the mean renal cortical NE levels decreased after combined denervation by 88.2% at 7 days and by 84.5% at 28 days. Liver NE decreased by 94.6% at 7 days and by 91.1% at 28 days (p<0.0001 for all) **(Figure 3, Central illustration)**. The variability in tissue NE samples was similar between the kidney and liver at both 7 days (p=0.16; F-test) and 28 days (p=0.15).

Vascular changes attributable to the procedure were morphologically consistent among renal and hepatic artery samples and characterised by segmental media and adventitial fibrosis. An anatomical classification of the number of tissue samples according to their relative location is summarised in **Supplementary Table 2**. The endothelial injury score was 0±0 in the hepatic and the left and right renal arteries at 7 and 28 days, indicating complete re-endothelialisation **(Figure 4)**. No thromboembolism or liver or renal infarct was observed in any tissue in either group. Hyalinisation (thermal denaturation) of collagen fibres was present around both the renal and hepatic arteries. Necrosis was minimal and restricted to the treated regions of the vessel at 7 days and was not observable at 28 days in either the renal or hepatic samples **(Figure 5)**. Fibrosis was apparent at both timepoints but was also restricted to the ablated regions of the vessel. Axonal loss (nerve atrophy) was present and extended distally beyond the treatment site at 7 and 28 days.

There was no evidence of significant thermal damage or injury to other renal or hepatic perivascular tissues, including the pancreas, duodenum, liver, bile duct, and

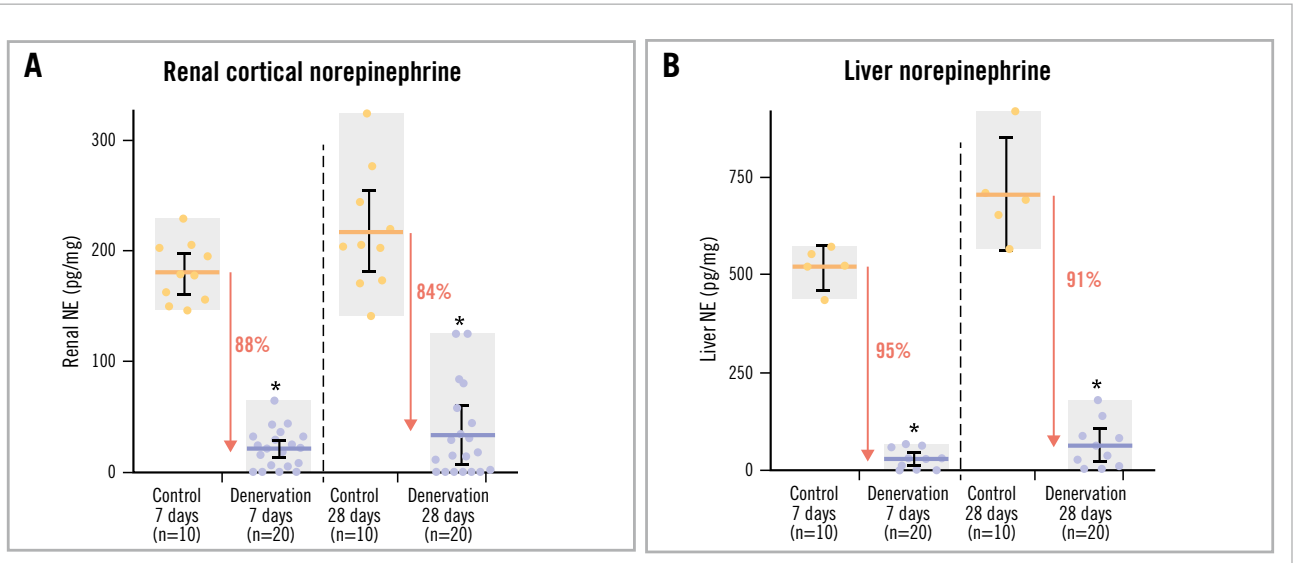

Figure 3. *NE concentrations in control and denervation cohorts. Renal cortical (A) and liver (B) tissue NE concentrations in combined renal and hepatic denervation and in untreated control cohorts of normotensive swine. Error bars: 95% confidence interval; grey boxes: range; horizontal bars: mean. *p<0.0001. NE: norepinephrine*

Combined bilateral renal denervation and common hepatic artery denervation using the multielectrode Symplicity Spyral catheter system.

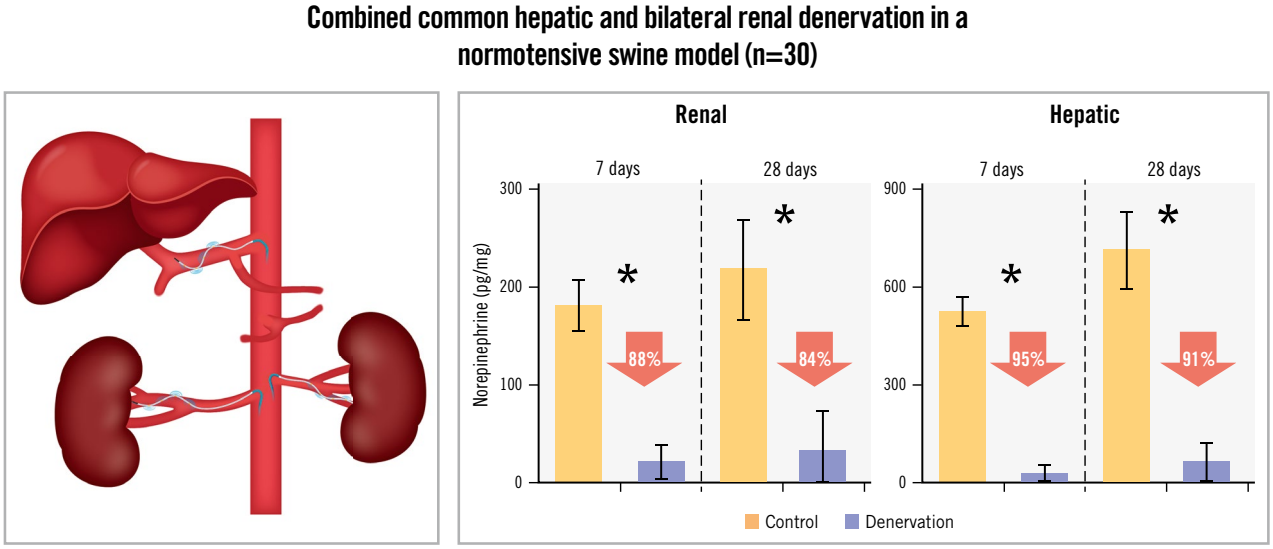

Felix Mahfoud *et al.* • *EuroIntervention* 2025;21:e1028-e1036 • DOI: 10.4244/EIJ-D-25-00349

*Both main vessel and primary branch renal arteries were treated. One catheter was used to treat all the vessels in each animal, and there was no evidence of significant thermal damage or injury to other renal or hepatic perivascular tissues. *p<0.0001*

kidneys, in either the 7-day or 28-day model **(Supplementary Table 3, Supplementary Table 4)**. Necrosis, thrombosis, and haemorrhage were minimally apparent in perivascular tissue at 7 days but not at 28 days, indicating normal progression of tissue healing. The mean inflammation and fibrosis scores specific to the ureter and pancreas tissue, respectively, were both minimal at 7 and 28 days despite their proximity to multiple ablation locations **(Supplementary Table 4)**. All untreated control perivascular tissues were morphologically normal.

Discussion

The main finding of this study was that combined ablation of both the renal and hepatic arteries was feasible, and safe in the short term, using an established RF RDN catheter system in this normotensive porcine model. The anatomical dimensions of the hepatic and renal arteries were comparable and compatible with the current U.S. FDA-approved RF RDN multielectrode catheter system[13]. However, the common hepatic periarterial nerves form a consistent multilayered plexus with less surrounding adipose tissue compared to that along the renal artery. Tissue NE reductions following RF denervation were substantial, consistent, and sustained at both 7 and 28 days post-procedure in the kidneys and the liver. Notably, the presently observed NE reductions were nominally greater in magnitude than those observed previously using the same model and the same ablation system after treatment of only the renal arteries[9]. Hence, the combination of renal and hepatic denervation may present an incremental and synergistic opportunity to reduce sympathetic nerve activity, although this hypothesis requires additional investigation[5].

Notably, collateral tissue damage was minimal and re-endothelialisation was complete by 7 days in the hepatic vessels, similar to the renal arteries. Tissue necrosis was limited to the treatment sites in both the hepatic and renal artery vessels and was fully resolved by day 28. However, fibrosis persisted and was confined to the treated vessel segments. In contrast, axonal loss extended distally beyond the treated vessel segments and persisted at 28 days. Together with sustained NE reductions, these data indicate a lack of functional nerve recovery in the short term and confirm a previous report of RF ablation in renal arteries[9].

It has previously been shown that coeliac ganglionectomy resulted in greater BP reductions compared to surgical RDN in a hypertensive rat model[14]. In addition, percutaneous RF denervation systems have been shown to be safe and effective in lowering BP in patients with uncontrolled hypertension with or without concomitant antihypertensive drug therapy up to 3 years of follow-up[15,16]. Observational studies through 10 years of follow-up after catheter-based RDN showed a durable effect without safety concerns[17-19]. The current study extends this knowledge, suggesting that an available RF system may be safely applied in both the renal and hepatic arteries, enabling multiorgan sympathetic denervation with one device.

The relative timing of histological analysis following treatment is important when considering these results.

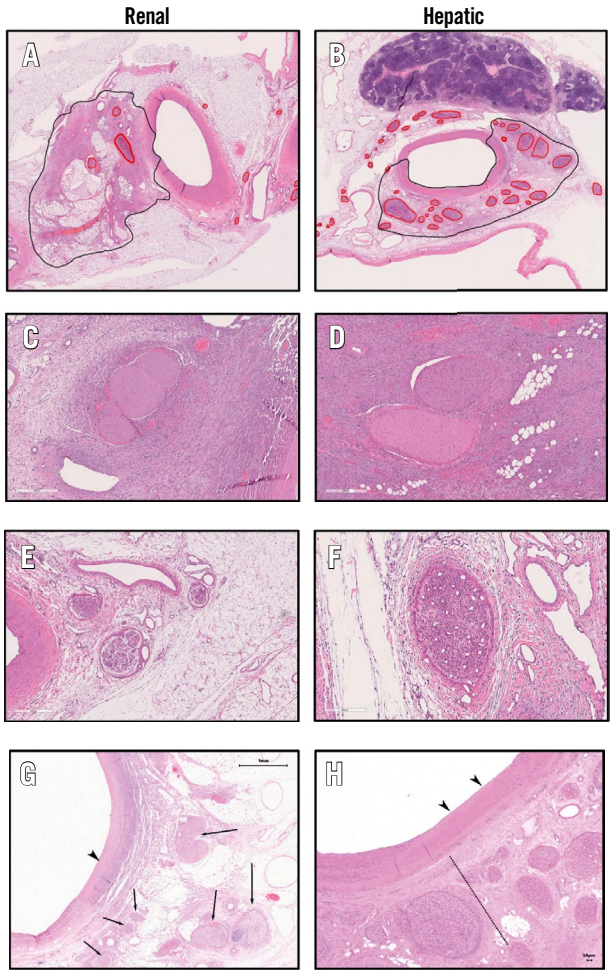

Figure 4. *Histological examples of nerve damage following renal and hepatic denervation. Histological examples of nerve damage following renal and hepatic denervation at 7 days including the main renal (A) and hepatic (B) arteries. RF-induced nerve necrosis at the site of ablation in the left renal artery (C) and common hepatic artery (D). Nerve atrophy distal to the site of renal (E) and hepatic (H) ablation. Site of electrode placement showing complete endothelialisation in the renal (G) and hepatic (H) arteries. Black arrowheads: media hyalinisation; nerves to the left of the dotted line show changes consistent with direct damage. Nerves to the right of the dotted line show changes consistent with atrophy. Arrows indicate direct nerve damage. RF: radiofrequency*

For example, we observed that the depth of RF tissue damage in the renal artery was significantly greater at 7 days than at 28 days. This is likely due to the ability of adipose tissue to gradually recover from thermal damage over several weeks following ablation, resulting in a decreased measured lesion depth over time. Interestingly, the presently reported renal artery lesion depths agree closely with two prior independent reports using the same ablation system in a similar porcine model at 7 days and 28 days, respectively[8,20]. In contrast to the renal arteries, the average lesion depth was similar at 7 and 28 days in the hepatic artery. This is likely due to less adipose tissue and more nerve tissue surrounding the hepatic artery than the renal arteries, which may result in a lesser influence of adipose healing on lesion depth in the hepatic arteries. Whether these anatomical differences in perivascular fat content translate into human vessels requires prospective investigation.

The mean circumferential extension of the ablated region around the vessel resulting from a single electrode was ≥33%, and the maximum extension was ≥59% in both the renal and hepatic arteries. Variability in the circumferential extension of the lesion is likely partly due to the presence and location of extravascular structures, such as lymph nodes and veins, acting as heat sinks and tanks relative to the lesion location[5]. Previous studies have shown that these tissues are distributed differently along the axis of the main renal artery[10] and the hepatic artery[5], respectively. Because of this variability, ablation along the entire axis of the CHA may also result in the most complete and least variable nerve destruction.

The clinical potential for multiorgan denervation might extend beyond lowering BP into other morbidities associated with overactivity of the sympathetic nervous system, such as cardiometabolic disease[21]. A qualitative comparison of renal and common hepatic artery tissue samples consistently showed more densely packed nerves surrounding the common hepatic artery. A recent preclinical study in a similar porcine model demonstrated substantial reductions in tissue NE in the kidney, liver, duodenum, and pancreas following combined renal and hepatic denervation using a dedicated balloon-based RF device in normotensive pigs[6]. Our results corroborate previous findings of human and porcine vessels showing that over 90% of nerves are within 5 mm of the hepatic artery lumen[21]. That study reported that the nerves were predominantly sympathetic efferent fibres, although some afferent fibres were also present. Therefore, combined renal and hepatic denervation may have effects beyond renal and hepatic function. Quantification of these potential benefits will require prospective clinical investigation. Tissue NE reduction is a well-established indicator of decreased sympathetic nerve activity. The histological results were limited to 28 days of follow-up. However, prior reports of RDN in the same model have shown durability to at least 180 days[9].

Limitations

The results of this study should be interpreted within the context of important limitations. The present analysis was conducted using a normotensive porcine model. Therefore, the impact on BP changes was not assessed. However, large animal models for induced hypertension are complex and differ from human hypertension and thus may not be suitable to meaningfully evaluate BP reductions. Likewise, human hepatic artery anatomy may vary compared to porcine anatomy[22]. Therefore, the effect of this combined sympathetic denervation on hypertensive patients must be evaluated in subsequent human trials such as the ongoing prospective SPYRAL GEMINI trial (ClinicalTrials.gov: NCT06907147).

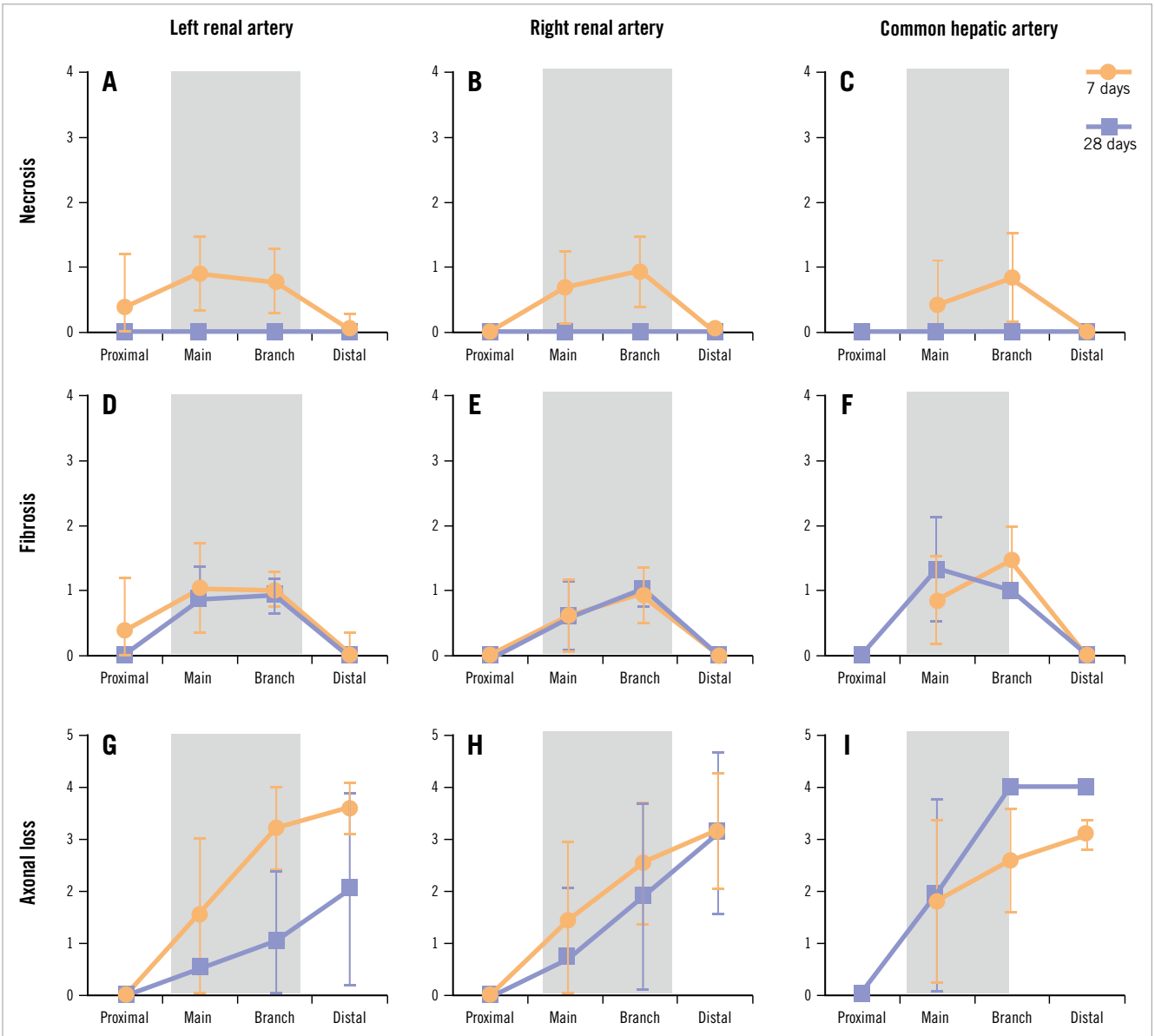

Figure 5. *Quantification of damage following denervation. Quantification of mean tissue necrosis (A-C), fibrosis (D-F), and nerve body axonal loss (G-I) in the common hepatic artery (right), left renal artery (left), and right renal artery (centre) at 7 (orange) and 28 (blue) days after radiofrequency renal denervation. Tissue samples were grouped by relative position including "proximal" to the aorta, "main" vessel, "branch" vessel, and "distal" to the ablation site. Grey shaded rectangles indicate the approximate location of the ablated area along the treated vessel axis. See* ***Supplementary Table 2*** *for details on scoring and number of tissue samples. Data are mean±standard deviation.*

Conclusions

In summary, combined hepatic and RDN using a single arterial access point, single device and generator, and the same energy level and treatment algorithm resulted in substantial reductions in both renal and hepatic tissue NE content that were sustained up to 28 days without collateral tissue damage. These mechanistic findings may have implications for the treatment of chronic diseases associated with hepatic and renal sympathetic nervous system overactivity. The ongoing SPYRAL GEMINI clinical programme will help determine the additional potential benefits of multiorgan denervation for BP lowering in patients with uncontrolled hypertension.

Authors' affiliations

1. Department of Cardiology, Department of Biomedical Engineering, and Department of Biomedicine, University Heart Center, University Hospital Basel, Basel, Switzerland; 2. Medtronic, Santa Rosa, CA, USA; 3. Department of Cardiology, Piedmont Heart Institute, Atlanta, GA, USA; 4. Division of Cardiology, Department of Medicine, Smith Center for Outcomes Research in Cardiology, Beth Israel Deaconess Medical Center, Boston, MA, USA and Harvard Medical School, Boston, MA, USA; 5. Division of Cardiovascular Medicine, Department of Medicine, University of California, San Diego, CA, USA; 6. Department of Medicine, Division of

Nephrology and Hypertension, University of North Carolina, Chapel Hill, NC, USA; 7. Dobney Hypertension Centre, Medical School – Royal Perth Hospital Unit and RPH Research Foundation, The University of Western Australia, Perth, WA, Australia and Department of Cardiology and Department of Nephrology, Royal Perth Hospital, Perth, WA, Australia

Acknowledgements

The authors thank Serge D. Rousselle, DVM, DACVP of StageBio, Frederick, MD, for technical assistance.

Funding

This study was funded by Medtronic, Inc.

Conflict of interest statement

F. Mahfoud has been supported by Deutsche Forschungsgemeinschaft (SFB TRR219, Project-ID 322900939), and Deutsche Herzstiftung. Saarland University has received scientific support from Ablative Solutions, Medtronic, and ReCor Medical. Until May 2024, F. Mahfoud received speaker honoraria/consulting fees from Ablative Solutions, AstraZeneca, Inari Medical, Medtronic, Merck, Novartis, Philips, and ReCor Medical. D.E. Kandzari has received institutional research/grant support from Biotronik, Boston Scientific, Cardiovascular Systems, Inc., OrbusNeich, Teleflex, Medtronic, and Ablative Solutions; and personal consulting honoraria from Cardiovascular Systems, Inc., Medtronic, and Abbott. E.A. Secemsky reports research funding from NIH from HLBI K23HL150290, U.S. Food & Drug Administration; institutional grants from Abbott, BD, Boston Scientific, Cook, Medtronic, and Philips; and consulting fees from Abbott, BD, Boston Scientific, Cook, Cordis, Endovascular Engineering, Gore, InfraRedx, Medtronic, Philips, RapidAI, Rampart, Shockwave Medical, Siemens, Teleflex, Terumo, Thrombolex, VentureMed, and Zoll. P.R. Taub has served as a consultant for Amgen, Bayer, Esperion, Boehringer Ingelheim, Novo Nordisk, and Sanofi; is a shareholder in Epirium Bio; and has received research grants from the NIH (R01 DK118278-01 and R01 HL136407), the American Heart Association (SDG #15SDG2233005), and the Department of Homeland Security/FEMA (EMW-2016-FP-00788). R.A. Voora is a paid consultant and speaker for Medtronic and Mineralys Therapeutics. L. Lauder has received speaker honoraria from AstraZeneca, Medtronic, Pfizer, and ReCor Medical. S. Tunev, D.A. Hettrick, C. Ryan, and D. Trudel are full-time employees of Medtronic. M. Schlaich has received institutional grants or contracts and personal consulting fees from Medtronic, Abbott, and ReCor Medical; personal payment or honoraria from Medtronic, Abbott, Merck, and Servier Laboratories; personal support for attending meetings, travel, or both from Medtronic and Abbott; serves as the President of the High Blood Pressure Research Council of Australia; and is on the International Society of Hypertension scientific committee.

References

1. Mancia G, Kreutz R, Brunström M, Burnier M, Grassi G, Januszewicz A, Muiesan ML, Tsioufis K, Agabiti-Rosei E, Algharably EAE, Azizi M, Benetos A, Borghi C, Hitij JB, Cifkova R, Coca A, Cornelissen V, Cruickshank JK, Cunha PG, Danser AHJ, Pinho RM, Delles C, Dominiczak AF, Dorobantu M, Doumas M, Fernández-Alfonso MS, Halimi JM, Járai Z, Jelaković B, Jordan J, Kuznetsova T, Laurent S, Lovic D, Lurbe E, Mahfoud F, Manolis A, Miglinas M, Narkiewicz K, Niiranen T, Palatini P, Parati G, Pathak A, Persu A, Polonia J, Redon J, Sarafidis P, Schmieder R, Spronck B, Stabouli S, Stergiou G, Taddei S, Thomopoulos C, Tomaszewski M, Van de Borne P, Wanner C, Weber T, Williams B, Zhang ZY, Kjeldsen SE. 2023 ESH Guidelines for the management of arterial hypertension The Task Force for the management of arterial hypertension of the European Society of Hypertension: Endorsed by the International Society of Hypertension (ISH) and the European Renal Association (ERA). *J Hypertens.* 2023;41:1874-2071.

2. McEvoy JW, McCarthy CP, Bruno RM, Brouwers S, Canavan MD, Ceconi C, Christodorescu RM, Daskalopoulou SS, Ferro CJ, Gerdts E, Hanssen H, Harris J, Lauder L, McManus RJ, Molloy GJ, Rahimi K, Regitz-Zagrosek V, Rossi GP, Sandset EC, Scheenaerts B, Staessen JA, Uchmanowicz I, Volterrani M, Touyz RM; ESC Scientific Document Group. 2024 ESC Guidelines for the management of elevated blood pressure and hypertension. *Eur Heart J.* 2024;45:3912-4018.

3. Cluett JL, Blazek O, Brown AL, East C, Ferdinand KC, Fisher NDL, Ford CD, Griffin KA, Mena-Hurtado CI, Sarathy H, Vongpatanasin W, Townsend RR; American Heart Association Council on Hypertension; Council on Cardiovascular and Stroke Nursing; Council on the Kidney in Cardiovascular Disease; and Council on Peripheral Vascular Disease. Renal Denervation for the Treatment of Hypertension: A Scientific Statement From the American Heart Association. *Hypertension.* 2024;81:e135-48.

4. Adori M, Bhat S, Gramignoli R, Valladolid-Acebes I, Bengtsson T, Uhlèn M, Adori C. Hepatic Innervations and Nonalcoholic Fatty Liver Disease. *Semin Liver Dis.* 2023;43:149-62.

5. Tzafriri AR, Garcia-Polite F, Keating J, Melidone R, Knutson J, Markham P, Edelman ER, Mahfoud F. Morphometric analysis of the human common hepatic artery reveals a rich and accessible target for sympathetic liver denervation. *Sci Rep.* 2022;12:1413.

6. Kiuchi MG, Ganesan K, Keating J, Carnagarin R, Matthews VB, Herat LY, Goh G, Adams L, Schlaich MP. Combined renal and common hepatic artery denervation as a novel approach to reduce cardiometabolic risk: technical approach, feasibility and safety in a pre-clinical model. *Clin Res Cardiol.* 2021;110:740-53.

7. Lauder L, Mahfoud F, Azizi M, Bhatt DL, Ewen S, Kario K, Parati G, Rossignol P, Schlaich MP, Teo KK, Townsend RR, Tsioufis C, Weber MA, Weber T, Böhm M. Hypertension management in patients with cardiovascular comorbidities. *Eur Heart J.* 2023;44:2066-77.

8. Mahfoud F, Tunev S, Ewen S, Cremers B, Ruwart J, Schulz-Jander D, Linz D, Davies J, Kandzari DE, Whitbourn R, Böhm M, Melder RJ. Impact of Lesion Placement on Efficacy and Safety of Catheter-Based Radiofrequency Renal Denervation. *J Am Coll Cardiol.* 2015;66:1766-75.

9. Sharp ASP, Tunev S, Schlaich M, Lee DP, Finn AV, Trudel J, Hettrick DA, Mahfoud F, Kandzari DE. Histological evidence supporting the durability of successful radiofrequency renal denervation in a normotensive porcine model. *J Hypertens.* 2022;40:2068-75.

10. Sato Y, Sharp ASP, Mahfoud F, Tunev S, Forster A, Ellis M, Gomez A, Dhingra R, Ullman J, Schlaich M, Lee D, Trudel J, Hettrick DA, Kandzari DE, Virmani R, Finn AV. Translational value of preclinical models for renal denervation: a histological comparison of human versus porcine renal nerve anatomy. *EuroIntervention.* 2023;18:e1120-8.

11. Sakakura K, Ladich E, Cheng Q, Otsuka F, Yahagi K, Fowler DR, Kolodgie FD, Virmani R, Joner M. Anatomic assessment of sympathetic peri-arterial renal nerves in man. *J Am Coll Cardiol.* 2014;64:635-43.

12. Mahfoud F, Tunev S, Ruwart J, Schulz-Jander D, Cremers B, Linz D, Zeller T, Bhatt DL, Rocha-Singh K, Böhm M, Melder RJ. Efficacy and safety of catheter-based radiofrequency renal denervation in stented renal arteries. *Circ Cardiovasc Interv.* 2014;7:813-20.

13. Lauder L, Kandzari DE, Lüscher TF, Mahfoud F. Renal denervation in the management of hypertension. *EuroIntervention.* 2024;20:e467-78.

14. Foss JD, Fink GD, Osborn JW. Reversal of genetic salt-sensitive hypertension by targeted sympathetic ablation. *Hypertension.* 2013;61:806-11.

15. Böhm M, Kario K, Kandzari DE, Mahfoud F, Weber MA, Schmieder RE, Tsioufis K, Pocock S, Konstantinidis D, Choi JW, East C, Lee DP, Ma A, Ewen S, Cohen DL, Wilensky R, Devireddy CM, Lea J, Schmid A, Weil J, Agdirlioglu T, Reedus D, Jefferson BK, Reyes D, D'Souza R, Sharp ASP, Sharif F, Fahy M, DeBruin V, Cohen SA, Brar S, Townsend RR; SPYRAL

HTN-OFF MED Pivotal Investigators. Efficacy of catheter-based renal denervation in the absence of antihypertensive medications (SPYRAL HTN-OFF MED Pivotal): a multicentre, randomised, sham-controlled trial. *Lancet*. 2020;395:1444-51.

16. Kandzari DE, Townsend RR, Kario K, Mahfoud F, Weber MA, Schmieder RE, Pocock S, Tsioufis K, Konstantinidis D, Choi J, East C, Lauder L, Cohen DL, Kobayashi T, Schmid A, Lee DP, Ma A, Weil J, Agdirlioglu T, Schlaich MP, Shetty S, Devireddy CM, Lea J, Aoki J, Sharp ASP, Anderson R, Fahy M, DeBruin V, Brar S, Böhm M; SPYRAL HTN-ON MED Investigators. Safety and Efficacy of Renal Denervation in Patients Taking Antihypertensive Medications. *J Am Coll Cardiol*. 2023;82:1809-23.

17. Sesa-Ashton G, Nolde JM, Muente I, Carnagarin R, Lee R, Macefield VG, Dawood T, Sata Y, Lambert EA, Lambert GW, Walton A, Kiuchi MG, Esler MD, Schlaich MP. Catheter-Based Renal Denervation: 9-Year Follow-Up Data on Safety and Blood Pressure Reduction in Patients With Resistant Hypertension. *Hypertension*. 2023;80:811-9.

18. Al Ghorani H, Kulenthiran S, Recktenwald MJM, Lauder L, Kunz M, Götzinger F, Ewen S, Ukena C, Böhm M, Mahfoud F. 10-Year Outcomes of Catheter-Based Renal Denervation in Patients With Resistant Hypertension. *J Am Coll Cardiol*. 2023;81:517-9.

19. Vogt A, Dutzmann J, Nußbaum M, Hoyer D, Tongers J, Schlitt A, Sedding D, Plehn A. Safety and efficacy of renal sympathetic denervation: a 9-year long-term follow-up of 24-hour ambulatory blood pressure measurements. *Front Cardiovasc Med*. 2023;10:1210801.

20. Wolf M, Hubbard B, Sakaoka A, Rousselle S, Tellez A, Jiang X, Kario K, Hohl M, Böhm M, Mahfoud F. Procedural and anatomical predictors of renal denervation efficacy using two radiofrequency renal denervation catheters in a porcine model. *J Hypertens*. 2018;36:2453-9.

21. Kiuchi MG, Carnagarin R, Matthews VB, Schlaich MP. Multi-organ denervation: a novel approach to combat cardiometabolic disease. *Hypertens Res*. 2023;46:1747-58.

22. Favelier S, Germain T, Genson PY, Cercueil JP, Denys A, Krausé D, Guiu B. Anatomy of liver arteries for interventional radiology. *Diagn Interv Imaging*. 2015;96:537-46.

Supplementary data

Supplementary Table 1. Semiquantitative scoring scales.

Supplementary Table 2. Total number of tissue samples analysed for necrosis, fibrosis, atrophy (axonal loss), and endothelialisation in all denervated animals.

Supplementary Table 3. Summary of damage to other perivascular tissues.

Supplementary Table 4. Summary of damage to ureter and pancreas.

Supplementary Figure 1. Determination of circumferential lesion extension.

The supplementary data are published online at: https://eurointervention.pcronline.com/doi/10.4244/EIJ-D-25-00349

Supplementary data

Supplementary Table 1. Semiquantitative scoring scales.

Endothelialization:
0: All endothelial cells are present
1: 75-95% of endothelial cells are present
2: 50-75% of endothelial cells are present
3: 25-50% of endothelial cells are present
4: <25% of endothelial cells are present

Necrosis and Fibrosis:
0: Not present
1: Present, minimal to mild
2: Mild to moderate
3: Moderate to severe

Atrophy (Score % affected):
0: No nerve atrophy identified
1: ~0-25% of nerve fascicles affected
2: ~25-50% of nerve fascicles affected
3: ~50-75% of nerve fascicles affected
4: ~75-100% of nerve fascicles affected

Supplementary Table 2. Total number of tissue samples analysed for necrosis, fibrosis, atrophy (axonal loss), and endothelialisation in all denervated animals.

Artery	Time	Proximal	Main	Branch	Distal
Left Renal	7 days	5	62	40	25
	28 days	11	60	43	41
Right Renal	7 days	6	90	33	23
	28 days	11	109	28	52
Common Hepatic	7 days	0	88	17	15
	28 days	12	106	1	17

Tissues were sectioned every 3-4 mm and sorted according to relative location. Proximal: near aorta; main: main treated vessel; branch: branch vessels including treated renal branches (Hepatic treatment was confined to the common hepatic artery only).

Supplementary Table 3. Summary of damage to other perivascular tissues.

	Inflammation	Necrosis	Fibrosis	Thrombus	Hemorrhage
Renal					
Day 7 (n=20)	1.1±0.1	1.0±0.2	1.0±0.2	0.5±0.2	0.8±0.2
Day 28 (n=20)	0.9±0.1	0.0±0.0	1.0±0.2	0.0±0.0	0.0±0.0
Hepatic					
Day 7 (n=10)	1.2±0.2	0.6±0.3	1.3±0.3	0.3±0.1	0.5±0.2
Day 28 (n=10)	1.4±0.2	0.0±0.0	1.6±0.2	0.0±0.0	0.0±0.0

Evidence of previous direct damage to perivascular tissues, including the ureter, lymph nodes and kidneys, or liver and pancreas, was characterized by fibrosis/fibrovascular tissue deposition and inflammation using semi-quantitative scoring (Supplemental table S1). Fibrosis with residual inflammation is the expected outcome after injury occurs to living tissue and it is part of nominal healing where there were no added complications (i.e., infection, abscesses, extensive tissue loss). Acute pancreatic necrosis was noted in animals from both treated and control groups. The acute nature of the change is consistent with perimortem autolysis, interpreted as non-treatment related (post-mortem artifact). All untreated control perivascular tissues were morphologically normal. (Data are mean ± SD).

Supplementary Table 4. Summary of damage to ureter and pancreas.

	Inflammation	Necrosis/Fibrosis	RF Treatments within examined section (n)
Ureter			
Day 7 (n=20)	0.0±0.0	0.0±0.0	3.2±0.8
Day 28 (n=20)	0.0±0.1	0.0±0.0	2.6±0.8
Pancreas			
Day 7 (n=10)	0.1±0.1	0.1±0.1	3.7±1.5
Day 28 (n=10)	0.0±0.1	0.1±0.1	3.2±1.0

Evidence of previous direct damage to the ureter and pancreas in the treated groups using semi-quantitative scoring (Supplemental table S1). All untreated control perivascular tissues were morphologically normal. (Data are mean ± SD; RF: radiofrequency)

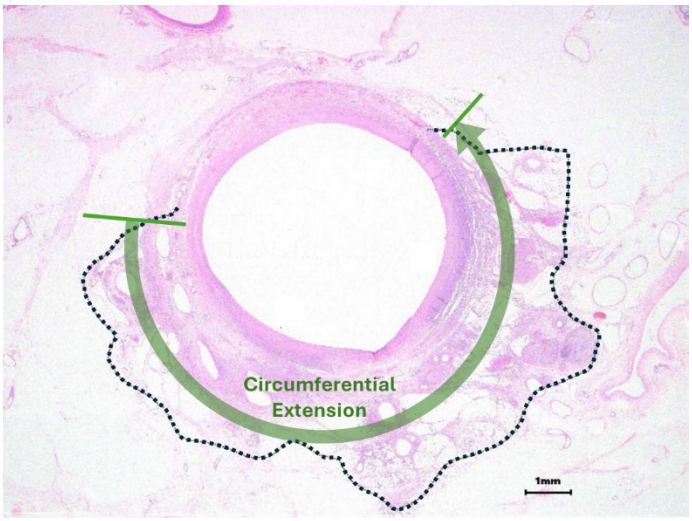

Supplementary Figure 1. Determination of circumferential lesion extension.

Circumferential extension within the perivascular space (green arrow) for this example renal artery was calculated as the percentage of the vessel circumference encompassed by the RF lesion (dashed line).